On the spatial sampling of wave fields with circular ring apertures

F. Simonetti, L. Huang, and N. Duric

Citation: J. Appl. Phys. **101**, 083103 (2007); doi: 10.1063/1.2717086
View online: http://dx.doi.org/10.1063/1.2717086
View Table of Contents: http://jap.aip.org/resource/1/JAPIAU/v101/i8
Published by the American Institute of Physics.

On the spatial sampling of wave fields with circular ring apertures

F. Simonetti[a)]
Department of Mechanical Engineering, Imperial College, London SW7 2AZ, United Kingdom

L. Huang
Los Alamos National Laboratory, MS D443, Los Alamos, New Mexico 87545

N. Duric
Karmanos Cancer Institute, Wayne State University, 4100 John R, Detroit, Michigan 48201

(Received 5 January 2007; accepted 4 February 2007; published online 20 April 2007)

This paper investigates the sampling criterion needed to image objects within a circular ring array. The array consists of transducer elements deployed along a circular aperture at regular angular intervals. Each transducer excites waves which propagate towards the center of the array and detects outgoing fields traveling towards it. It is shown that while with conventional linear apertures the sampling criterion is dictated by the wavelength of the probing wave only, in the case of a circular aperture the sampling depends on the size of the object relative to the wavelength and its position with respect to the aperture. © *2007 American Institute of Physics*. [DOI: 10.1063/1.2717086]

I. INTRODUCTION

A number of imaging methods are based on the measurement of wave fields either radiating from a source or scattered by an object. A typical imaging scenario is depicted in Fig. 1 in which a probing wave is incident on the object to be imaged and the scattered field is measured along an aperture. In the vast majority of imaging applications such as medical diagnostics, radar surveillance, geophysical exploration, and nondestructive testing, the aperture is a line or a plane depending on whether two- or three-dimensional imaging is required. The field is measured either with a single sensor scanned along the aperture or with an array of transducers which covers the entire aperture. For a monochromatic wave field, the minimum spatial interval between consecutive sampling points depends on the wavelength λ of the field. In particular, in order to retrieve the whole information content carried by the field, the interval should be smaller than $\lambda/2$ according to the Shannon sampling theorem.[1] Larger sampling intervals lead to artifacts in the reconstructed images known as grating lobes, whereas oversampling does not add extra information and results in a more complicated array architecture.

The question arises whether the Shannon sampling criterion should also be used for circular apertures. The class of circular apertures considered in this paper refers to ring arrays consisting of transducer elements deployed along a circular ring at regular angular intervals. Each array element excites waves propagating towards the center of the array and detects outgoing waves radiating from the center of the aperture (Fig. 1). Thanks to recent progress in solid state electronics ring arrays with hundreds or even thousands of elements have been manufactured for ultrasound tomography.[2–5] In this context, an accurate definition of the sampling criterion would help in defining the right balance between image quality and minimum number of sensors. Indeed, Lin *et al.*[3] have already proposed a sampling criterion for imaging circular cylinders. In this paper, their results are generalized to cylindrical objects with arbitrary cross section and the conditions under which the criterion is applicable are discussed. Moreover, the structure of the grating lobes is investigated and compared to that of the grating lobes of linear arrays.

Section II reviews the sampling theory for linear apertures and provides the framework on which the sampling criterion for a circular aperture is derived in Sec. III.

II. LINEAR APERTURE

Conventional imaging methods produce an image of an object by illuminating it from one or more directions and recording the scattered field at different positions in space by means of an array of sensors. The image is reconstructed by backprojecting or migrating the measured field into a *virtual* background medium in an attempt to reconstruct the field everywhere in the probed region. In ultrasound tomography, the illumination is carried out by exciting a transient wave of short duration. In the framework provided by Fourier analysis the transient can always be thought of as a superposition of monochromatic waves with frequencies ranging within the

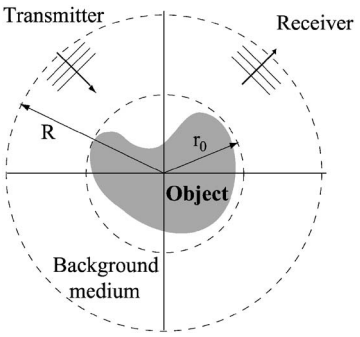

FIG. 1. A plane wave is incident on an object immersed in a homogeneous background medium. The field scattered by the object is measured with sensors placed in the far field.

[a)]Electronic mail: f.simonetti@imperial.ac.uk

bandwidth of the transient. For this reason in the rest of this paper only monochromatic waves are considered, unless differently specified.

Let us consider a two-dimensional wave field, a set of Cartesian coordinates $\{O,x,z\}$, and a linear aperture along the line $z=0$. Let $f(x)$ be the complex wave field, scattered by an object and detected along the aperture. The spatial Fourier transform of $f(x)$, $F(k_x)$, can be expressed as

$$f(x) = \int_{-\infty}^{+\infty} dk_x F(k_x) e^{ik_x x}. \tag{1}$$

According to the angular spectrum method,[6] the backprojected field at any point in space can be thought of as the superposition of infinite, elementary plane waves, $\psi(x,z)$,

$$\psi(x,z) = dk_x F(k_x) e^{ik_x x} e^{ik_z z}, \tag{2}$$

where k_z is given by

$$k_z = \begin{cases} \sqrt{k^2 - k_x^2}, & k_x < k \\ i\sqrt{k_x^2 - k^2}, & k_x > k, \end{cases} \tag{3}$$

and $k=2\pi/\lambda$ is the wave number of the background medium. The condition $k_x > k$ corresponds to evanescent waves which decay within one wavelength distance from the aperture.

Let us now consider the simple case of a plane wave field impinging on a linear aperture at normal incidence. If the field could be measured along all the points of an infinitely wide aperture, the angular spectrum $F(k_x)$ would be a Dirac delta function centered at $k_x=0$ and the backprojected field would correspond to a single plane wave orthogonal to the aperture, so providing an exact reconstruction of the incident field. However, in practice the size of the aperture and the sampling interval are limited; therefore the backprojected field differs from the original plane wave leading to artifacts. The artifacts can be studied by analyzing the spectrum of the actual measurements, which can be expressed as $f(x) = p(x)g(x)$, where $p(x)$ is the pupil function defining the extent and apodization of the aperture and $g(x)$ is a periodic function such that

$$g(x + n\Delta) = g(x), \quad \forall\, n \in \mathbb{Z}, \tag{4}$$

where $\mathbb{Z}$ is the set of integer numbers and Δ represents the sampling interval. The spectrum of $f(x)$ is the convolution of the Fourier transform of the pupil function $P(k_x)$ and that of $g(x)$, $G(k_x)$. Since $g(x)$ is a periodic function with period Δ, it can be expanded in a Fourier series,

$$g(x) = \sum_{n=-\infty}^{n=+\infty} a_n e^{ink_0 x}, \tag{5}$$

where a_n are coefficients which depend on the size of each sensor and $k_0 = 2\pi/\Delta$. The Fourier transform of Eq. (5) gives

$$G(k_x) = \sum_{n=-\infty}^{n=+\infty} a_n \delta(k - nk_0), \tag{6}$$

where $\delta(\cdot)$ is the Dirac delta. As an example, Fig. 2 shows the modulus of $F(k_x)$ for an aperture with a square pupil function,

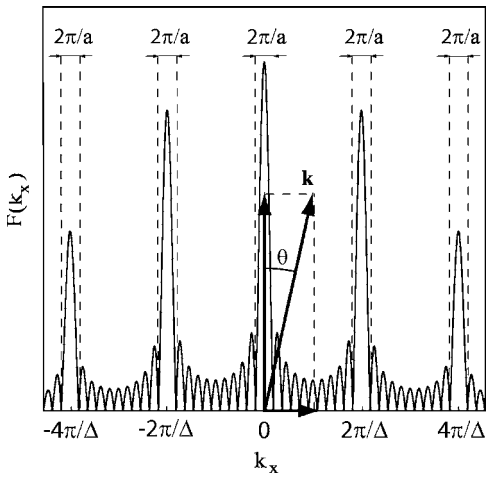

FIG. 2. Amplitude of the angular spectrum of a uniform field measured with a sampling period Δ along a linear aperture of size $2a$. The wave number k_x defines the propagation direction ϑ of the elementary plane waves according to the vector diagram.

$$p(x) = \begin{cases} 1, & |x| < a \\ 0, & |x| > a, \end{cases} \tag{7}$$

where $2a$ is the length of the aperture. Since the Fourier transform of $p(x)$ is

$$P(k_x) = \frac{2\sin(k_x a)}{k_x}, \tag{8}$$

the convolution with $G(k_x)$ leads to periodic peaks whose width is $2\pi/a$ and which are spaced $2\pi/\Delta$ apart. The width of the lobes only depends on the size of the aperture which also determines the amplitude of the neighboring side lobes, whereas the position of the peaks is defined by the sampling interval only. Clearly, this spectrum is very different from the one which would be obtained with an infinite aperture and continuous sampling along it, i.e., $\delta(k_x)$. Using the angular spectrum method, $F(k_x)$ can be backprojected by integrating the contributions from all the plane waves associated with $F(k_x)$. The peaks produce larger radiation in the directions corresponding to $k_x = nk_0$ (see vector diagram in Fig. 2), which result in the presence of so called *grating lobes* in the reconstructed field. The angle between the grating lobes and the normal to the aperture θ_n is given by

$$\sin(\theta_n) = n\frac{\lambda}{\Delta}, \quad \forall\, n \in \mathbb{Z}. \tag{9}$$

For instance, Fig. 3 shows the amplitude of the field radiating from five point sources equally spaced along an aperture of size 10λ ($\Delta = 2.5\lambda$), the sources having the same phase and amplitude. This situation corresponds to the field backprojected by the aperture when the incident field is a plane wave at normal incidence. The large value of Δ leads to grating lobes which occur at $\pm 23.6°$ and $\pm 53.1°$, as predicted by Eq. (9).

In Eq. (9) the condition $n\lambda/\Delta > 1$ corresponds to the case in which $k_x > k$, for which the plane waves are evanescent and decay within one wavelength distance from the aperture. As a result, even if the spectrum has maxima for $k_x > k$, they do not contribute to the total field far from the

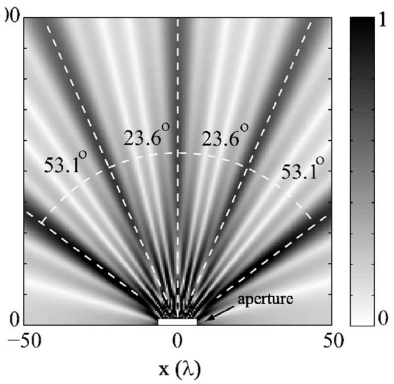

FIG. 3. Amplitude of the backprojected field corresponding to an incident plane wave perpendicular to an aperture of size 10λ and a sampling interval of $\Delta=2.5\lambda$. The field was obtained as a superposition of the fields radiated by point sources located at the sampling points, the sources having the same amplitude and phase. Due to the large sampling spacing the reconstructed field contains grating lobes at ±23.6° and ±53.1°.

aperture. In order to avoid the appearance of grating lobes in the reconstructed field the sampling interval should be such that

$$\Delta < \lambda. \tag{10}$$

The condition $\Delta=\lambda$ corresponds to grating lobes parallel to the aperture [see Eq. (9)]. Criterion (10) holds when the incident wave is orthogonal to the aperture, in the more general case of a plane wave incident at an angle β, the spectrum $F(k_x)$ is shifted by $k_x \sin\beta$ and the first pair of grating lobes occurs at

$$\sin\theta_1 = \sin\beta + \frac{\lambda}{\Delta}, \tag{11}$$

$$\sin\theta_2 = \sin\beta - \frac{\lambda}{\Delta}. \tag{12}$$

As a result, grating lobes can be avoided by ensuring that the right hand sides of Eqs. (11) and (12) are always larger than 1, leading to the standard Shannon sampling theorem,

$$\Delta < \lambda/2. \tag{13}$$

As a last remark, it should be noticed that if the aperture were infinitely wide, condition (13) would ensure a perfect reconstruction of the field since the field reaching the aperture is band limited ($|k_x|<2\pi/\lambda$) due to the fact that the propagation medium (from the object to the aperture) acts as a low pass filter which suppresses the spatial frequencies larger than $2\pi/\lambda$.[6]

III. CIRCULAR APERTURE

Let us now consider a system of cylindrical coordinates $\{O,\theta,\rho\}$ with origin at the center of a circular aperture of radius R (Fig. 1), θ and ρ being the azimuthal and radial coordinates, respectively. The partial wave expansion of a wave field $\psi(\theta,\rho)$ in cylindrical coordinates is

$$\psi(\theta,\rho) = \sum_{n=-\infty}^{+\infty} [A_n H_n^{(1)}(k\rho) + B_n H_n^{(2)}(k\rho)] e^{in\theta}, \tag{14}$$

where $H_n^{(1)}$ and $H_n^{(2)}$ are the nth order Hankel functions of the first and second kinds, respectively, and A_n and B_n are constants. Each term of the expansion is a solution to the Helmholtz equation $(\nabla^2+k^2)\psi(\theta,\rho)=0$ and $H_n^{(1)}$ and $H_n^{(2)}$ are waves propagating outward and inward, respectively. The field reaching the aperture is given by

$$f(\theta) = \sum_{n=-\infty}^{+\infty} [A_n H_n^{(1)}(kR) + B_n H_n^{(2)}(kR)] e^{in\theta}, \tag{15}$$

and its Fourier series expansion is the discrete spectrum,

$$F(n) = A_n H_n^{(1)}(kR) + B_n H_n^{(2)}(kR), \tag{16}$$

where $n \in \mathbb{Z}$ is the angular wave number.

As for the linear aperture, let us consider the simple case in which the field reaching the aperture is independent of θ. This situation can occur when the wavelength of the illuminating wave is much larger than the object size, and the object is located at the center of the aperture. In this case, the scattered field radiates symmetrically with respect to the center of the aperture. Because of the symmetry, only the coefficient A_0 in the expansion (15) is nonzero whereas B_0 vanishes because it corresponds to an inward wave. If the field is sampled with N equally spaced sensors, the measured spectrum is

$$F(n) = a_n, \quad \forall\, n \in \{0, \pm N, \pm 2N, \ldots\} \tag{17}$$

where the coefficients a_n depend on the size of the sensors as in (6). Using the same argument which leads to the angular spectrum method, the field obtained by backprojecting the signal recorded by each sensor, $\psi_b(\theta,\rho)$ is equivalent to the field given by (14). The coefficients A_n and B_n are obtained by equating (16) and (17) and ensuring that $\psi_b(\theta,\rho)$ is nonsingular within the area enclosed by the aperture, thus

$$A_n = B_n = \frac{a_n}{2J_n(kR)}, \quad \forall\, n \in \{0, \pm N, \pm 2N, \ldots\} \tag{18}$$

where $J_n(\cdot)$ is the nth order Bessel function of the first kind and the Hankel function property $H_n^{(1)}(kR)+H_n^{(2)}(kR)=2J_n(kR)$ has been used. As a result, the backprojected field is a standing wave given by

$$\psi_b(\theta,\rho) = \sum_{m=-\infty}^{+\infty} a_{mN} \frac{J_{mN}(k\rho)}{J_{mN}(kR)} e^{imN\theta}, \tag{19}$$

the expansion is extended to all the angular wave numbers which are integer multiples of the number of sampling points N. For a linear aperture it was observed that only the plane waves with wave number $k_x<k$ contribute to the field since for $k_x>k$ the plane waves are evanescent and decay within one wavelength distance from the aperture. A dual argument holds for expansion (19). In particular, the Bessel functions $J_n(\cdot)$ exhibit both an evanescent and an oscillatory behaviors depending on the value of their argument and the order n. As an example, Fig. 4 shows the Bessel function $J_{32}(\cdot)$. The function has a maximum at $k\rho=\gamma_{32}=34.6$, which marks the

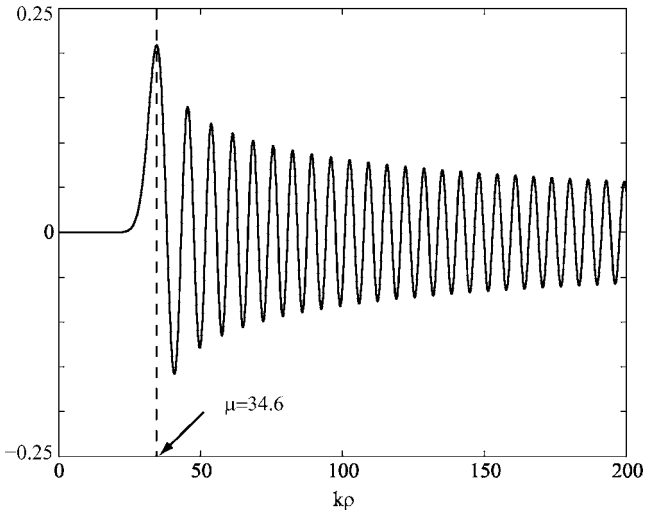

FIG. 4. Bessel function of the first kind and order 32. For $k\rho<34.6$ the function is evanescent while for $k\rho>34.6$ it becomes oscillatory.

transition from evanescent to oscillatory behavior. The physical implication of the transition is that if the series (19) contains the term $J_n(\cdot)$, this will not contribute to the field within a circle of radius $\rho_t<\gamma_n/k$. The value of γ_n depends on the order of the Bessel function, as shown in Fig. 5, which provides the ratio $\alpha_n=\gamma_n/n$ for different orders n; note that in the limit for large n, α_n tends to 1. Since the backprojected field is the superposition of all the Bessel functions of order nN, it will contain maxima which occur along the circles of radii,

$$R_n = \alpha_{nN}\frac{|n|N}{k}, \quad \forall\, n \in \mathbb{Z}, \tag{20}$$

so producing circular grating lobes. As an example, Fig. 6 shows the amplitude of the field radiating from 100 point sources equally spaced along a circular aperture of radius 50λ all having the same amplitude and phase. Three grating lobes occurring along the circles of radii, 16.5λ, 32.6λ, and 48.6λ, can be observed, as predicted by Eq. (20). By comparing Fig. 3 with Fig. 6 it can be observed that while for a linear aperture the grating lobes span the field of view linearly, in the case of a circular aperture the field is spanned angularly.

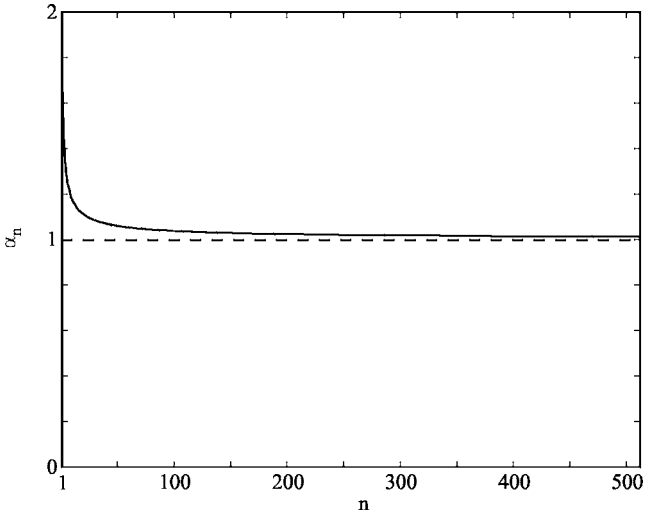

FIG. 5. Ratio α_n for different values of the the Bessel function order. For large orders the ratio tends to 1.

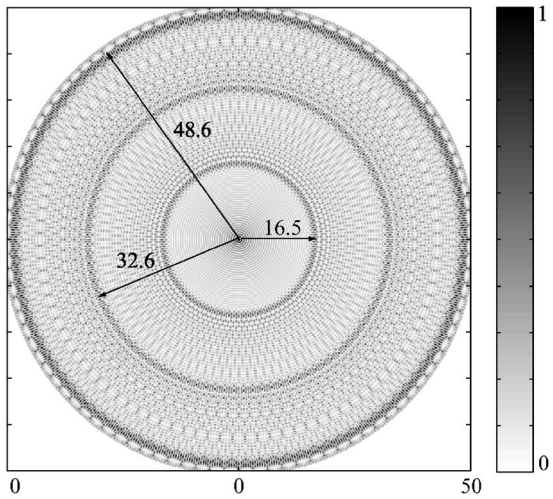

FIG. 6. Amplitude of the backprojected field corresponding to an incident cylindrical wave radiating from the center of a circular aperture of radius 50λ and with 100 sampling points equally spaced. The field was obtained as the superposition of the fields radiating from 100 point sources located at the sampling points. The dimensions are given in λ.

To avoid grating lobes within the area enclosed by the aperture, the first grating lobe R_1 should occur outside the aperture, hence the condition $R_1>R$ along with (20) gives

$$\Delta < \alpha_N\lambda, \tag{21}$$

where Δ is the arc length between two adjacent sampling points.

Expression (21) has been derived under the assumption that the field reaching the aperture is uniform; in fact, only the order zero was considered in the expansion (14). The result can now be generalized to the case in which the detected field has order l, either positive or negative. This is the realistic scenario in which the object is probed with a wavelength which is not much larger than the object size. In this case the spectrum (17) is shifted by l and the new grating lobes are defined by

$$R_n = \alpha_{nN+l}\frac{|nN+l|}{k}, \quad \forall\, n \in \mathbb{Z}. \tag{22}$$

Note that the backprojected field is still represented by Eq. (19), where the index mN is replaced by $mN+l$. As a result, the first pair of grating lobes occurs at

$$R_{-1} = \alpha_{|N-1|}\frac{|N-l|}{k}, \tag{23}$$

$$R_{+1} = \alpha_{|N+l|}\frac{|N+l|}{k}. \tag{24}$$

The grating lobe with the smallest radius depends on the largest (smallest) order l which can reach the aperture. In order to define an upper bound for $|l|$, the propagation mechanism of a wave field from the object to the aperture has to be studied.

For this purpose let us consider the field $v(\theta)$ in the near zone of the object along the circle of radius r_0 which circumscribes the object (see Fig. 1). In general the field will contain all the outgoing terms appearing in the expansion (15). The field which travels from the circle of radius r_0 to a larger circle of radius ρ is

$$\psi(\theta,\rho) = \sum_{n=-\infty}^{+\infty} v_n \frac{H_n^{(1)}(k\rho)}{H_n^{(1)}(kr_0)} e^{in\theta}, \tag{25}$$

where

$$v_n = \int_0^{2\pi} d\theta v(\theta) e^{-in\theta}. \tag{26}$$

Now it can be observed that when the argument of a Hankel function is larger than its order, i.e., $kr_0 > n$, the function has asymptotic form[7]

$$H_n^{(1)}(kr_0) \approx \sqrt{\frac{2}{\pi kr_0}} e^{i[kr_0 - n(\pi/2) - (\pi/4)]}, \tag{27}$$

so leading to

$$\frac{H_n^{(1)}(k\rho)}{H_n^{(1)}(kr_0)} \approx \sqrt{\frac{r_0}{\rho}} e^{ik(\rho - r_0)}, \tag{28}$$

which implies that all the orders $n < kr_0$ propagate to the far field. This also suggests that the fluctuations of the field $v(\theta)$ along the circle of radius r_0 with a circumferential period $\Delta_\theta > \lambda$ can reach the far field. Now consider the condition $n > kr_0$. In this case the asymptotic form of the Hankel function becomes

$$H_n^{(1)}(kr_0) \approx \frac{1}{n!}\left(\frac{kr_0}{2}\right)^n - i\frac{(n-1)!}{\pi}\left(\frac{2}{kr_0}\right)^n, \tag{29}$$

where for large n, the real part is negligible compared to the imaginary one, thus

$$\frac{H_n^{(1)}(k\rho)}{H_n^{(1)}(kr_0)} \approx \left(\frac{r_0}{\rho}\right)^n. \tag{30}$$

As a result, the fluctuations of $v(\theta)$ characterized by $\Delta_\theta < \lambda$ $(n > kr_0)$ do not reach the far field because their amplitudes decay with the nth power of the radial coordinate ρ rather than its square root as in Eq. (28).

Therefore, the upper bound for $|l|$ is dictated by the characteristic size of the object r_0 and is given by

$$\sup\{|l|\} < kr_0. \tag{31}$$

Now that the upper bound has been defined, the sampling criterion can be derived by imposing that the first grating lobe occurs outside the region in space which contains the object, i.e., the circle of radius r_0 (see Fig. 1). By substituting (31) into (23) the minimum number of sampling points is

$$N > \frac{2\pi r_0}{\lambda}\left(1 + \frac{1}{\alpha_{N-1}}\right) \approx \frac{4\pi r_0}{\lambda}, \tag{32}$$

which means that the separation distance between the sensors deployed along a circular aperture of radius R has to satisfy the condition

$$\Delta < \frac{\lambda R}{2r_0}. \tag{33}$$

Criterion (33) is the extension of the standard sampling theorem (13) to the case of a circular aperture and is equivalent to the condition introduced by Lin *et al.*[3] for circular scatterers. This expression is consistent with the sampling criterion for linear apertures. In fact, for a linear aperture, the $\lambda/2$ sampling criterion ensures that the entire field of view is imaged free of artifacts, i.e., the object can be of any size and in any location in space. If the same has to be achieved with the circular aperture, then r_0 has to be the same as R so as to remove any constraint on the size and position of the object to be imaged. In this case (33) becomes the same as (13).

It has to be emphasized that (33) has been derived under the assumption that R is sufficiently larger than r_0 so that $(r_0/R)^n$ is negligible for any order $(n > kr_0)$, thus ensuring that high order components of the wave field are filtered by the background medium and condition (31) holds. On the other hand, when r_0 approaches R, it is no longer possible to define an *a priori* upper bound and aliasing can occur even if (33) is satisfied. Moreover, criterion (33) requires that the object to be imaged is contained within the circle of radius r_0 concentric with the aperture. If the object is contained within a circle of radius r_0, C_1, which is not concentric, the upper bound will be defined based on the radius of the concentric circle of radius $r > r_0$ which inscribes C_1, resulting in a larger N. Therefore, the sampling criterion depends on the characteristic size of the object relative to the wavelength and its position with respect to the aperture.

It can be observed that condition (33) can be relaxed if prior knowledge about the object shape and properties of its boundary can ensure that the largest order l is lower than that given by (31). As an example, if the surface of the object is smooth and its reflectivity is low, the contribution of the partial waves of order close to kr_0 will be negligible compared to that of the partial waves generated by more pronounced features close to the core of the object. In this context, r_0 in expression (33) can be replaced with an effective radius $r_{\text{eff}} < r_0$, which identifies the region of the object which is more active in scattering the incident field.

Although the analysis performed in this paper has considered monochromatic waves, it can be generalized to the case in which the probing wave is a pulse by means of standard Fourier analysis. As a result, the backprojected field is the superposition of the monochromatic backprojected fields corresponding to the frequencies within the bandwidth of the probing wave. Depending on the spectral content of the wave packet, different wavelengths can cause the grating lobes to interfere constructively or destructively, thus enhancing or attenuating the amplitude of the grating lobes.

IV. CONCLUSIONS

This paper has investigated a spatial sampling criterion for imaging objects within a circular ring array consisting of transducers deployed along a circular aperture. While with conventional linear arrays it is sufficient to use a sampling interval smaller than half of the wavelength according to the

Shannon sampling theorem, in the case of a circular aperture the sampling interval depends on the size of the object to be imaged relative to the wavelength and on its position with respect to the aperture. This is due to the fact that the size and position of the object determine the maximum circumferential order of the field which reaches the aperture.

ACKNOWLEDGMENTS

This work was supported through the U.S. DOE Laboratory-Directed Research and Development program at Los Alamos National Laboratory. One of the authors (F.S.) is also grateful to the UK Royal Academy of Engineering/ Engineering and Physical Sciences Research Council for supporting this work.

[1] A. J. Jerri, Proc. IEEE **65**, 1565 (1977).
[2] M. P. Andre, H. S. Janee, P. Martin, G. P. Otto, B. A. Spivey, and D. A. Palmer, Int. J. Imaging Syst. Technol. **8**, 137 (1997).
[3] F. Lin, A. I. Nachman, and R. C. Waag, J. Acoust. Soc. Am. **108**, 899 (2000).
[4] F. Simonetti, L. Huang, and N. Duric (unpublished).
[5] R. C. Waag and R. J. Fedewa, IEEE Trans. Ultrason. Ferroelectr. Freq. Control **53**, 1707 (2006).
[6] J. W. Goodman, *Introduction to Fourier Optics* (McGraw-Hill, New York, 1996).
[7] G. B. Arfken and H. J. Weber, *Mathematical Methods for Physicists* (Academic, London, 2001).